

# Quantum meets classical phase transition: Low-temperature anomaly in disordered superconductors near $B_{c2}$

Johanna Seidemann,<sup>1,2</sup> Benjamin Sacépé,<sup>1,2,\*</sup> Maoz Ovadia,<sup>3</sup>  
Dan Shahar,<sup>3</sup> Karen Michaeli,<sup>3</sup> and Mikhail V. Feigel'man<sup>4,5</sup>

<sup>1</sup>*Univ. Grenoble Alpes, Institut Néel, F-38000 Grenoble, France*

<sup>2</sup>*CNRS, Institut Néel, F-38000 Grenoble, France*

<sup>3</sup>*Department of Condensed Matter Physics, The Weizmann Institute of Science, Rehovot 76100, Israel.*

<sup>4</sup>*L. D. Landau Institute for Theoretical Physics, Chernogolovka, 142432, Moscow region, Russia*

<sup>5</sup>*National Research University "Higher School of Economics", Moscow, Russia*

Strongly disordered superconductors in a magnetic field display many characteristic properties of type-II superconductivity—except at low temperatures where a significant upturn of the critical field  $B_{c2}$  with a linear  $T$ -dependence is routinely observed. This behavior violates the conventional theory of superconductivity, and its origin remains a long-standing puzzle. Here we report on systematic measurements of the critical magnetic field and current on amorphous indium oxide films of various levels of disorder. Surprisingly, our measurements show that the  $B_{c2}$  upturn near zero-temperature is accompanied by a clear mean-field like scaling behavior of the critical current. We demonstrate theoretically that these are consequences of the vortex-glass ground state and its thermal fluctuations. This theory further predicts the linear- $T$  anomaly to occur in films as well as bulk superconductors with a slope that depends on the normal-state sheet resistance—in agreement with experimental data. Thus, our combined experimental and theoretical study reveals universal low-temperature behavior of  $B_{c2}$  in a large class of disordered superconductors.

The magnetic-field tuned transition of disordered superconductors continues to surprise as well as to pose intriguing and challenging puzzles. A wealth of experimental results obtained over decades of study still defies current theoretical understanding. The anomalous temperature dependence of the critical field  $B_{c2}(T)$  near the quantum critical point between superconductor and normal metal is a well known example. Within the conventional Bardeen-Cooper-Schrieffer theory,  $B_{c2}(T)$  is expected to saturate at low temperatures [1, 2]. In contrast, a strong upturn of  $B_{c2}$  with a *linear- $T$*  dependence as  $T \rightarrow 0$  has been observed in numerous disordered superconductors. These systems range from alloys and oxides, both in thin films [3–9] and bulk [10], to boron-doped diamond [11] as well as gallium monolayers [12].

Substantial theoretical efforts [13–17] have been unable to fully resolve the origin of this anomalous behavior. The main challenge lies in the complexity of these systems and the subtle interplay between strong fluctuations, disorder and vortex physics. The prevailing explanation for the low- $T$  anomaly of  $B_{c2}(T)$  is based on mesoscopic fluctuations [13, 14], which result in a spatially inhomogeneous superconducting order parameter. A recent alternative interpretation invokes a quantum Griffiths singularity to account for the upturn in  $B_{c2}(T)$  observed in ultra-thin gallium films [12]. While these theoretical approaches are generally plausible, they predict an exponential increase of  $B_{c2}(T)$  at very low  $T$ , which manifestly does not capture the specific *linear* dependence measured in disordered superconductors [3–12].

To gain new insights on the underlying physical mechanism it is desirable to not only study  $B_{c2}(T)$ , but to also extract information on additional characteristic quanti-

ties such as the superfluid stiffness. We therefore conducted systematic measurements of both  $B_{c2}$  and the critical current  $j_c$  in thin films of amorphous indium oxide (a:InO), a prototypical disordered superconductor. In the absence of magnetic field or when vortices are strongly pinned by disorder (i.e., form a vortex glass) the superfluid stiffness can be directly related to the critical current. This is expected to apply to all materials that exhibit the low-temperature upturn of  $B_{c2}$  [3–12]. Consequently, measurements of  $j_c(B)$  near zero temperature provide access to the critical behavior of the superfluid density  $\rho_s(B)$  near  $B_{c2}(0)$ , where the low- $T$  anomaly develops.

In this work we show that the linear  $T$ -dependence of  $B_{c2}(T)$  at low temperatures is accompanied by a *power-law* dependence of the critical current on  $B$ . The critical exponent of  $j_c(B) \sim |B - B_{c2}|^v$  is found to be  $v \simeq 1.6$ . As explained below, this is consistent with the mean field value  $v = 3/2$  (but not with the mesoscopic fluctuation scenario [13, 14] which predicts an exponential dependence [14]). Our unexpected finding has direct implication for the critical behavior of  $\rho_s(B)$ , and demands a revised theory of disordered superconductors in the presence of magnetic field. We therefore complement our experimental work with a comprehensive theoretical study, which identifies the key to understanding the linear  $T$ -dependence of  $B_{c2}$  in the vortex glass. When vortices are strongly pinned by impurities, their presence only weakly affects the  $T = 0$  limit of superfluid stiffness and critical current. As a result, both exhibit mean-field-like dependence on the magnetic field. In contrast, the temperature variation of the superfluid stiffness is strongly affected by thermal fluctuations of the vortex glass. This

gives rise to the observed linear  $T$ -dependence of  $B_{c2}(T)$  near the quantum critical point. Moreover, we predict a strong dependence of the slope  $dB_{c2}(T)/dT|_{T \rightarrow 0}$  on the sheet resistance, and consequently on the film thickness, which we confirm experimentally.

## Results

**Disordered superconducting thin-films.** Disordered a:InO films were prepared by e-gun evaporation of 99.99 %  $\text{In}_2\text{O}_3$  pellets on a Si/SiO<sub>2</sub> substrate in a high-vacuum chamber with a controlled O<sub>2</sub> partial pressure. Films were patterned into Hall bar geometry (300  $\mu\text{m}$  long and 100  $\mu\text{m}$  wide) by optical lithography, enabling four-terminal transport measurements using standard low-frequency lock-in amplifier and DC techniques. The magneto-transport properties of the samples upon varying disorder are presented in our previous work [9]. In this study we mainly focus on two samples J033 and J038, which exhibit a critical temperature of  $T_c = 3.2$  K and 3.5 K and a sheet resistance before transition of  $1.3 \text{ k}\Omega$  and  $1.2 \text{ k}\Omega$  respectively. They are both far from the disorder-tuned superconductor-insulator transition and behave in many ways as standard dirty superconductors.

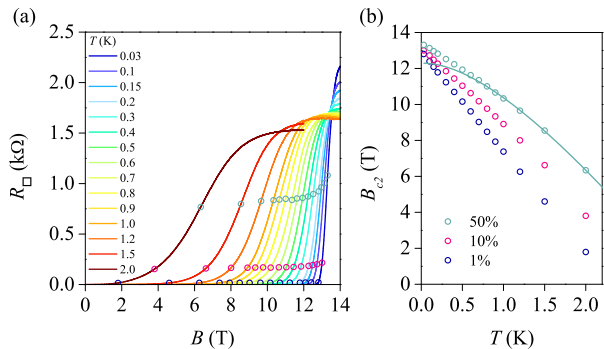


FIG. 1: **Low- $T$  anomaly of the upper critical field  $B_{c2}(T)$ .** (a)  $R_{\square}$  versus  $B$  measured at fixed temperatures for sample J033. Open circles indicate the determination of  $B_{c2}(T)$  using three different criteria, namely 50, 10 and 1% of the high field normal state resistance. (b) Extracted  $B_{c2}(T)$  values from the measurement shown in (a), plotted versus  $T$ . The solid line is a high temperature fit using the theory for dirty superconductors [1, 2].

**Low- $T$  anomaly near  $B_{c2}(0)$ .** Figure 1(a) displays the magneto-resistance isotherms of sample J033 measured down to 0.03 K. To determine  $B_{c2}$  at each temperature we used three different criteria, namely 1, 10 and 50% of the normal state resistance at high field, indicated by open dots on magneto-resistance isotherms. The resulting  $B_{c2}$  versus  $T$  curves are shown in Fig. 1(b) together with a fit (solid-line) of the high-temperature data with the theory for dirty superconductors [1, 2]. We

see that  $B_{c2}(T)$  deviates below  $\lesssim 1$  K from the fit and increases linearly with decreasing  $T$  down to our base temperature of 0.03 K. This deviation, which is the focus of this work, is independent of the criterion used to determine  $B_{c2}$ .

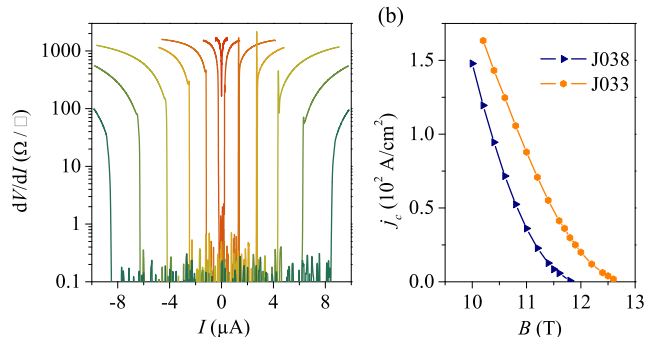


FIG. 2: **Critical current density  $j_c$  near  $T = 0$  and  $B_{c2}(0)$ .** (a)  $dV/dI$  versus  $I$  of sample J033 measured at  $T = 0.03$  K and at magnetic fields of 10.4, 10.8, 11.2, 11.6, 12, 12.5 and 13 T (green to red curves respectively). (b)  $j_c$  versus  $B$  of both samples J033 and J038. Each values of  $j_c(B)$  were extracted from  $dV/dI$  versus  $I$  measurements as shown in (a) at the resistance value of  $dV/dI = 10 \Omega/\square$ .

An important aspect of the linear dependence of  $B_{c2}(T)$  is that it persists down to our lowest  $T$  approaching the quantum phase transition QPT at  $B_{c2}(0)$ . We shall argue below that the linear dependence of  $B_{c2}(T)$  can be understood by analyzing the critical behavior of the superfluid density in the vicinity of this QPT.

### Critical regime of the critical current density.

We turn to the study of the  $B$ -evolution of the critical current density  $j_c$  at our lowest temperature. We systematically measured the differential resistance  $dV/dI$  versus current-bias  $I$  at fixed  $B$ 's. As shown in Fig. 2(a), on increasing  $I$ , a sudden, non-hysteretic jump occurs in the  $dV/dI$  curve, indicating the critical current value. The resulting critical current density  $j_c$  for both samples is plotted versus  $B$  in Fig. 2(b). Interestingly, the continuous suppression of  $j_c$  with increasing  $B$  tails off prior to vanishing at a critical field  $B_c^{jc} = 12.6 \text{ T}$  and  $11.8 \text{ T}$  for sample J033 and J038 respectively. Such a resilience of  $j_c$  to the applied  $B$  when approaching  $B_{c2}(0)$  is reminiscent of the anomalous upturn of the  $B_{c2}(T)$  line at low  $T$ . We also notice that the critical field values  $B_c^{jc}$  at which  $j_c$  vanishes slightly differ from  $B_{c2}(0)$  obtained in Fig 1 ( $B_{c2}(0) = 13.3 \text{ T}$  and  $12.6 \text{ T}$  determined with the 50 % criterion for sample J033 and J038 respectively). The reasons for this disparity stem from the finite-resistance criterion used to determine  $B_{c2}(T)$ , which does not coincide with the termination of superconducting current at  $B_c^{jc}$ .

The key result of this work is shown in Fig. 3 where  $j_c$  is plotted in logarithmic scale as a function of  $|B_c^{jc} - B|$ . By adjusting the value of  $B_c^{jc}$  in the x-axis to 12.8

and 11.9 T for samples J033 and J038 respectively, one obtains clear straight lines that unveil a scaling relation of the form:

$$j_c \propto |B_c^{j_c} - B|^\nu, \quad (1)$$

where the fitted values for the exponent  $\nu$  are  $1.62 \pm 0.02$  and  $1.65 \pm 0.02$  for samples J033 and J038 respectively. The inset of Fig. 3 shows the sensitivity of the straight line to  $B_c^{j_c}$ , where a small variation of 0.05T yields a significant deviation from linearity. It is noteworthy that the values of the exponent are both within 10% of the mean-field value  $3/2$  of the classical temperature-driven superconducting transition in the absence of magnetic-field. Ginzburg-Landau theory predicts that the critical current would be  $j_c^{GL} \propto \rho_s / \xi_{GL} \propto (T_c - T)^{3/2}$ , with the Ginzburg-Landau superconducting coherence length  $\xi_{GL} \propto (T_c - T)^{-1/2}$  and  $\rho_s \propto (T_c - T)$ . This striking similarity suggests that also the scaling of  $B_{c2}(T)$  and  $j_c(B)$  low temperature may be captured by mean-field theory of the bulk material.

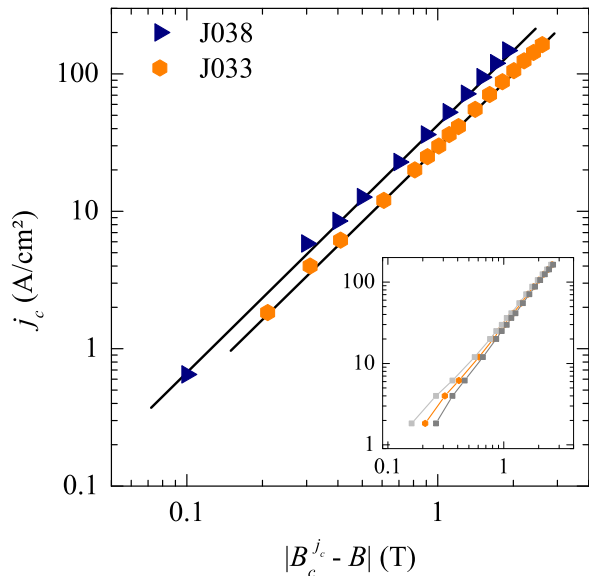


FIG. 3: **Scaling of the critical current density with magnetic field.**  $j_c$  versus  $|B_c^{j_c} - B|$ . The  $B_c^{j_c}$  values are adjusted to obtain straight lines that are emphasized by black solid-lines. Inset: the dark grey and light grey curves are plotted with  $B_c^{j_c} \pm \delta$ , where  $\delta = 0.05$  T.

**Interpretation of experimental results within mean-field theory.** The mean-field critical exponent of  $j_c(B)$  at  $T = 0$  near  $B_{c2}(0)$  can be extracted from the Ginzburg-Landau free energy which reads:

$$F = \alpha |\Delta(\mathbf{r})|^2 + \beta |\Delta(\mathbf{r})|^4 + \gamma \left| \left( -i\nabla - \frac{2e}{\hbar c} \mathbf{A}(\mathbf{r}) \right) \Delta(\mathbf{r}) \right|^2. \quad (2)$$

Within mean-field theory, the coefficient  $\alpha$  strongly de-

pends on temperature and magnetic field [18]:

$$\alpha = \nu \left[ \ln \frac{T}{T_{c0}} + \psi \left( \frac{1}{2} + \frac{eDB}{2\pi\hbar cT} \right) - \psi \left( \frac{1}{2} \right) \right]. \quad (3)$$

Here,  $D$  and  $\nu$  are the electron diffusion coefficient and density-of-states respectively, and  $\psi(x)$  is the digamma function.  $B$  in Eq. (3) is the magnetic field penetrating the superconductor. While for type-II superconductors such as our a:InO films this magnetic field can be non-uniform at low  $B$ , close to  $B_{c2}$  the spatial fluctuations of  $B$  are negligible, and the average magnetic field is equal to the externally applied one. The other two parameters of the Ginzburg-Landau functional,  $\beta$  and  $\gamma \propto \nu D$  depend only weakly on temperature and magnetic field. Consequently, Eq. (2) captures the two effects of magnetic field on superconductors: The suppression of the transition point due to pair-breaking (through the parameter  $\alpha$ ), and the diamagnetic response captured by the vector potential  $\mathbf{A}$ . Note that the expression for  $\alpha$  in Eq. (3) is typical for superconductors in the presence of a pair-breaking mechanism [19]. For example, the effect of magnetic impurities can be captured by replacing the magnetic field by a term proportional to the spin relaxation rate  $\Gamma$  [1]. Correspondingly, these systems have the same  $T = 0$  critical exponents (i.e.  $\alpha \approx |1 - B/B_{c2}|$  or analogously  $\alpha \approx |1 - \Gamma/\Gamma_c|$ ).

The  $T = 0$  limit of Eq. (2) yields the magnetic-field dependence of the order parameter and the coherence length near the quantum critical point,  $|\Delta(B)| \approx |B - B_{c2}|^{1/2}$  and  $\xi_{GL}(B) \approx |B - B_{c2}|^{-1/2}$ . The latter, together with the superfluid stiffness  $\rho_s$ , determines the mean-field value of the critical current:  $j_c^{GL} \propto \rho_s / \xi_{GL}$ . To find the superfluid stiffness, we match the superconducting current extracted from the free energy,  $\mathbf{j} = -c\partial F / \partial \mathbf{A}$ , with the London equation,  $\mathbf{j} = -4\rho_s e^2 \mathbf{A} / \hbar^2 c$ . We find that

$$\rho_s(B) = \frac{12}{\pi} \rho_{s0} \left( 1 - \frac{B}{B_{c2}(0)} \right), \quad (4)$$

and

$$j_c^{GL} \propto \rho_s / \xi_{GL} \sim |B - B_{c2}|^{3/2}. \quad (5)$$

The corresponding critical exponent  $\nu = 3/2$  is in excellent agreement with our experimental findings.

To complete the comparison between the experimental results and mean-field theory, we extract the low-temperature critical field from the condition  $\alpha(B, T) = 0$ . We find  $B_{c2}(0) - B_{c2}(T) \sim T^2$ , which is inconsistent with the linear dependence  $B_{c2}(0) - B_{c2}(T) \sim T$  that is observed experimentally (see Fig. 2). This discrepancy indicates that beyond-mean-field effects are important. In particular, Ginzburg-Landau theory does not include thermal fluctuations of the vortex-glass, which are essential in the finite-temperature transition to the normal state. As we will show below, these fluctuations are

the key ingredient to understanding the linear upturn of  $B_{c2}$ ; however, they do not change the scaling behavior of  $j_c(B, 0)$ .

**Vortex-glass fluctuations.** In low-dimensional superconductors the pairing instability is known to differ from the onset of phase coherence. A prominent example is the Berezinskii-Kosterlitz-Thouless (BKT) transition in thin films [20, 21]. Similar decoupling is known to occur in moderately-disordered type-II superconductors near  $B_{c2}$ , where the magnetic field gives rise to the formation of a weakly pinned vortex lattice [22, 23]. There, the transition temperature is determined by the vortex-lattice melting transition [24]  $T_c \propto (1 - B/B_{c2}(0))^2$ , which sets in well below the mean-field one. Moreover, the superconducting state becomes resistive when the force applied on the vortex lattice by the current exceeds the pinning forces. The corresponding depinning critical current  $j_c^{\text{depin}}$  is then significantly lower than the pair-breaking critical current extracted from the Ginzburg-Landau theory,  $j_c^{\text{GL}}$ .

In contrast, in highly disordered superconductors such as our a:InO films, we expect a vortex-glass [23, 25] rather than a lattice. In such a vortex-glass state the local fluctuations are gapped [26–28], and the strong pinning forces lead to a large depinning critical current such that  $j_c^{\text{GL}} \lesssim j_{\text{depin}}$ . As a consequence, eq. (5) still applies even in the presence of vortices. However, vortex-glass state fluctuations lead to a suppression of the superfluid stiffness [25] and an ensuing reduction of  $T_c$ . As we will show below, this is crucial for understanding the upturn of  $B_{c2}$  at low- $T$ .

To estimate the effect of vortex-glass fluctuations on  $\rho_s$ , which we anticipate to be well below the pairing instability, we focus exclusively on phase-fluctuations of the order parameter, i.e.  $\Delta(\mathbf{r}) = |\Delta_0|e^{i\Phi(\mathbf{r})}$ . Inserting this into this into the free energy, Eq. (2), yields  $F[\Phi] = \rho_s [\nabla\Phi(\mathbf{r}) - \frac{2e}{\hbar c}\mathbf{A}(\mathbf{r})]^2/2$ . It is convenient to further separate  $\Phi(\mathbf{r})$  into smooth phase fluctuations (the superfluid mode)  $\varphi(\mathbf{r})$  with  $\nabla \times \nabla\varphi = 0$  and fluctuations of the vortex-glass  $\psi(\mathbf{r})$ , with  $\Phi(\mathbf{r}) = \varphi(\mathbf{r}) + \psi(\mathbf{r})$ . We determine the renormalized superfluid stiffness via the static current-current correlation function  $\langle J_{\text{sc}}^i(\mathbf{r}, \omega_n = 0) \rangle = \int d\mathbf{r} \langle J_{\text{sc}}^i(\mathbf{r}, 0) J_{\text{sc}}^j(0, 0) \rangle A^j(0, 0)$ , where as before  $\mathbf{J}_{\text{sc}}(\mathbf{r}) = -c\partial F/\partial\mathbf{A}(\mathbf{r})$ . Since  $\rho_s$  is determined by the long-wavelength properties, it is sufficient to focus on length-scales larger than the (typical) inter-vortex spacing  $a_0$ . Moreover, within such a coarse-grained description, the coupling between superfluid and vortex fluctuations is local.

We note that a charge encircling a vortex acquires phases from both the external and the vortex field,  $\oint[\nabla\psi(\mathbf{r}) - 2e/\hbar c\mathbf{A}(\mathbf{r})] \cdot d\mathbf{l}$ . If the vortices were uniformly spaced (a vortex lattice), the two contributions to the phase would cancel at a length scale  $a_0$ . In the coarse grained description and in the symmetric gauge

for the vector potential, this amount to  $\nabla\psi(\mathbf{r}) = \mathbf{A}(\mathbf{r})$ . In a vortex-glass this cancellation is not exact. Still, near  $B_{c2}$  and at the length scales of  $a_0 = \sqrt{\Phi_0/B} \approx \xi_0\sqrt{2\pi}$ , the density of vortices is nearly uniform. We introduce the field  $\mathbf{R}(\mathbf{r}) = (R_x(\mathbf{r}), R_y(\mathbf{r}))$  that describes the deviation of the vortex positions from uniformity.  $\mathbf{R}$  thus encodes the particular realization of the vortex-glass, and, in the absence of forces, its spatial average vanishes,  $V^{-1} \int d\mathbf{r} \mathbf{R}(\mathbf{r}) = 0$ . It is thus appropriate to expand

$$\begin{aligned} \nabla\psi(\mathbf{r} - \mathbf{R}(\mathbf{r})) - \frac{2e}{\hbar c}\mathbf{A}(\mathbf{r}) &\approx -\frac{2e}{\hbar c}(\mathbf{R}(\mathbf{r}) \cdot \nabla)\mathbf{A} \quad (6) \\ &= \frac{\mathbf{u}(\mathbf{r}) \times \hat{z}}{2a_0}. \end{aligned}$$

where  $\mathbf{u}(\mathbf{r}) = 2\pi\mathbf{R}(\mathbf{r})/a_0$  is the dimensionless displacement field. It follows that the leading coupling terms in the free energy between  $\varphi$  and  $\mathbf{u}$  are

$$\delta F = \rho_s a_0^{-1} \hat{z} \cdot [\nabla\varphi(\mathbf{r}) \times \mathbf{u}(\mathbf{r})] - C\rho_s (\nabla\varphi(\mathbf{r}))^2 \mathbf{u}^2(\mathbf{r}), \quad (7)$$

where  $C$  is a material specific coefficient of order unity. Note that here we assume isotropy in the  $x - y$  plane.

The first term in Eq. (7) corresponds to the lowest order expansion with respect to gradients in the Ginzburg-Landau free energy (2). It gives rise to a temperature and magnetic-field independent correction to the superfluid stiffness that depends on the realization of the vortex-glass. This reduction enters the measurable quantity  $\rho_{s0}$  which we treat as a phenomenological parameter. As we show below, higher-order gradients (like the second term in Eq. (7)) become important at non-zero temperature. The leading contribution of such terms to  $\rho_s$  is given by

$$\delta\rho_s^{x,y} = -\frac{C\rho_s T}{a_0^3} \sum_n \int d\mathbf{r} \langle \mathbf{u}(\mathbf{r}, \omega_n) \cdot \mathbf{u}(0, -\omega_n) \rangle. \quad (8)$$

It remains to evaluate the  $\mathbf{u} - \mathbf{u}$  correlation function.

Our key hypothesis for describing the dynamics of the vortex-glass is that, at low temperature, it is governed by the motion of individual vortices around their respective pinning centers. Moreover, we assume that elasticity along the vortex line is negligible at distances beyond  $a_0$ . Thus, the equation of motion for  $\mathbf{u}(\mathbf{r}, t)$  can be deduced from the known behavior of an isolated vortex [23]. We find

$$\eta\partial_t\mathbf{u}(\mathbf{r}, t) + \kappa(\mathbf{u}(\mathbf{r}, t) - \mathbf{u}_0(\mathbf{r})) = \mathbf{f}(t) \equiv \frac{\hbar a_0}{2e} \mathbf{j} \times \hat{z}, \quad (9)$$

where  $\mathbf{u}_0(\mathbf{r})$  is the static displacement at zero current. The r.h.s. of Eq.(9) is the Lorentz force acting on a segment of a vortex of length  $a_0$  in presence of a supercurrent  $\mathbf{j}$ . We emphasize the absence of gradients of  $\mathbf{u}$  in the equation of motion—this manifests the locality of the vortex dynamics. Effectively, the vortex fluctuations in

the glass state at low temperature resemble a (damped) optical phonon mode. The parameter

$$\eta = (h/2e)^2 \sigma_n / 2\pi = \frac{\pi \hbar^2}{2e^2} \sigma_n$$

reflects the presence of normal electrons in the vortex cores, whose resistance  $\sigma_n^{-1}$  gives friction to the vortex motion (note that we defined friction coefficient  $\eta$  w.r.t. dynamics of dimensionless coordinate  $\mathbf{u} = 2\pi \mathbf{R}/a_0$ ). For strongly disordered materials  $\sigma_n a_0 \sim e^2/\hbar$  and thus  $\eta \sim \hbar/a_0$ . This overdamped character of the vortex motion leads us to neglect the inertial term  $\propto \partial_t^2 \mathbf{u}$  with respect to friction. Likewise, we neglect the contribution to the Lorentz force due to vortex velocity since it does not affect the relevant current-current correlation function. The parameter  $\kappa$  can be determined similar to the penetration length in pinned vortex systems, also known as the Campbell length [26–28] (for a recent review see Ref. [29]). According to Eq.(9), the shift of  $\mathbf{u}$  due to current  $\mathbf{j}$  is equal to  $\mathbf{u}(\mathbf{r}) - \mathbf{u}_0(\mathbf{r}) = \hbar a_0 (\mathbf{j} \times \mathbf{n}) / 2e\kappa$ . The corresponding shift of the vortex magnetic flux can be expressed through  $\delta \mathbf{A} = -\hbar \Phi_0 \mathbf{j} / 4e\kappa a_0$ . Using the London relation, we get  $\kappa = \pi \rho_s$ . From Eq. (9) we obtain the Matsubara Green's function of  $\mathbf{u}$

$$G(\mathbf{r}, \omega_n \neq 0) = a_0^2 \delta(\mathbf{r}) [\eta |\omega_n| + \kappa]^{-1}. \quad (10)$$

We thus arrive at the reduction of the superfluid stiffness due to thermal fluctuations of the vortex-glass. Combining Eqs. (8) and (10) yields the following correction to the superfluid stiffness:

$$\begin{aligned} \delta \rho_s(T, B) - \delta \rho_s(0, B) &= -C \frac{\rho_s(B)}{a_0} \left[ T \sum_n [\eta |\omega_n| + \kappa]^{-1} \right. \\ &\quad \left. - \int \frac{d\omega}{2\pi} [\eta |\omega| + \kappa]^{-1} \right] = -C \frac{\hbar \sigma_n}{e^2} \frac{T^2}{3\pi \rho_s(B) a_0}. \end{aligned} \quad (11)$$

The last equality holds in the low-temperature limit  $T/\hbar \ll \kappa/\eta$ ; in the opposite limit one recovers the classical result  $\langle \mathbf{u}^2 \rangle = T/\kappa$ . The smallness of the low temperature result  $\rho_s(T, B) \propto T^2$  is compensated by the small  $\rho_s(B) \propto 1 - B/B_{c2}(0)$  in the denominator, see Eq.(4). This new result is unique for disordered superconductors, in which the fluctuations at  $T > 0$  are controlled by the dissipation in the gapless vortex cores, and it provides the key to understanding the low- $T$  linear upturn of  $B_{c2}$ .

**Theory for the low-temperature anomaly.** We now apply this result to film as well as bulk superconductors. In the former, the transition temperature is set by the BKT condition:

$$\rho_s(B, T_{\text{BKT}}) = \chi T_{\text{BKT}}/d, \quad (12)$$

where  $d$  is the film thickness and  $\chi^{-1}$  was numerically found [30] to be between 1.5 to 2.2 (this holds for *any*

*value of  $d$*  [30–33]). Moreover, kinetic inductance measurements of thin a:InO films have unveiled a universal jump in the two-dimensional superfluid density per square even in the presence of a magnetic field, indicating that the BKT transition persists near the quantum critical point [34]. Combining the BKT condition with the renormalized  $\rho_s$  given by Eq. (11) yields:

$$1 - \frac{B_{c2}(T)}{B_{c2}(0)} = \left[ 1 + \sqrt{1 + C_1^2 \frac{d^2}{a_0^2}} \right] \frac{\pi \chi T}{24 \rho_{s0} d}, \quad (13)$$

where  $C_1^2 = 4C\hbar\sigma_n a_0 / 3\pi\chi^2 e^2$  is of order unity for our a:InO films. We thus obtain a linear temperature dependence of  $B_{c2}(T)$  at low  $T$ , which provides a theoretical description of our experimental data shown in Fig. 1b. In addition, this result is in agreement with numerous experiments in films [3–9, 12] and bulk [10, 11] disordered superconductors.

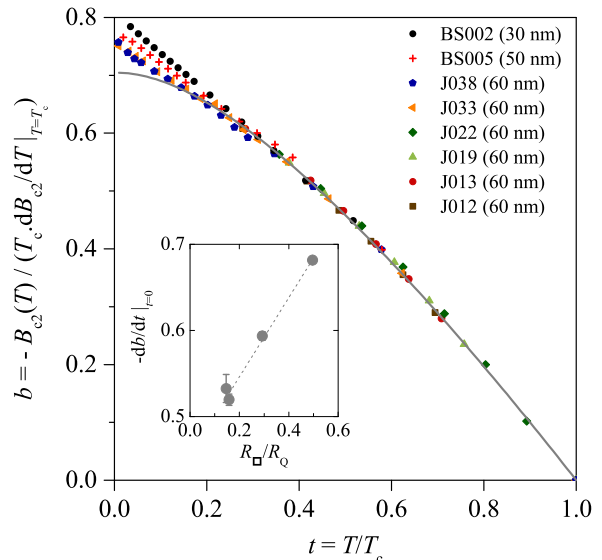


FIG. 4: **Disorder dependence of the low- $T$  anomaly.** (a)  $b = B_{c2}(T)/(-T_c dB_{c2}/dT|_{T=T_c})$  versus reduced temperature  $t = T/T_c$  for 8 samples of different thicknesses. The solid gray line is a fit using the mean field theory for dirty superconductors emphasizing the deviations at low  $T$ . Inset: Slope  $-db/dt$  at zero temperature versus  $R_{\square}/R_Q$ .

We emphasize that the linear upturn of  $B_{c2}(T)$  does not depend on the sample dimensionality and, in particular, remains valid for bulk superconductors. For films,  $|\delta \rho_s(B, T)/\rho_s(B)|$  grows with the film thickness  $d$ , but remains smaller than unity for finite  $d$ . Consequently, the assumptions entering Eq. (13) are well justified in the thin-film limit  $d \ll a_0$  (such as the experimental data reported in Ref. [12]). There, our theory predicts that the slope  $-dB_{c2}(T)/dT$  grows linearly with  $(\rho_{s0}d)^{-1}$ . For thicker films, however,  $|\delta \rho_s(B, T)/\rho_s(B)|$  increases and higher order corrections to  $\rho_s(B)$  can become important. Still,  $dB_{c2}(T)/dT|_{T \rightarrow 0}$  maintains the structure

$(\rho_{s0}a_0)^{-1}(g_0 + g_1a_0/d)$  with numerical coefficients  $g_{0,1}$  that (may) deviate from those given in Eq. (13). To conclude, while our analysis provides an exact expression for the slope only in the thin-film limit, it predicts a distinct  $d$ -dependence that holds for any thickness.

Finally, we provide a quantitative comparison between the theoretical prediction and experimental data from eight samples of various thicknesses and resistances. Experimentally, the physical parameters controlling the low-temperature linear deviation are difficult to assess directly from the  $B_{c2}(T)$  curves. The reduction of  $T_c$  and increase of  $B_{c2}(0)$  upon increasing sheet resistance leads to an apparent increase of the slope  $dB_{c2}/dT|_{T \rightarrow 0}$  in the  $B - T$  plane (see fig. 2(b) in ref. 9). This makes a direct comparative analysis between different samples impossible. The non-universal dependence of  $T_c$  and  $B_{c2}(0)$  on disorder can be eliminated by considering the quantity  $b(t) = B_{c2}(T)/(-T_c dB_{c2}/dT|_{T=T_c})$  versus the reduced temperature  $t = T/T_c$ . Figure 4 displays  $b(t)$  for the eight different samples together with the theoretical mean-field curve, in solid line, found by setting  $\alpha$  to zero [1, 2]. We see that, for  $t \gtrsim 0.2 - 0.3$ , all high-temperature data collapse on the theoretical curve. At smaller  $t$ , the low-temperature anomaly of  $B_{c2}$  develops as a linear deviation from the mean-field curve. Our theory explains the anomalous slope in this regime and, as we show below, captures the dependence on the sample parameters.

To compare the plot in Fig. 4 with our theory, we extract  $b(t)$  from Eq. (13) and find:

$$-\frac{db}{dt} = \begin{cases} KR_{\square}/R_Q & d \ll a_0 \\ \tilde{g}_0 \sqrt{\frac{1}{\sigma_n R_Q a_0}} + \tilde{K} \frac{R_{\square}}{R_Q} & d \gg a_0 \end{cases}, \quad (14)$$

where  $R_Q = h/4e^2$  is the quantum of resistance for electron pairs (for details see Supp. Info.). Neglecting higher order corrections to  $\rho_s$  beyond Eq. (13), and the suppression of  $\rho_{s0}/T_{c0}$  in strongly disordered superconducting films yields  $K = 0.4\pi \approx 1$ ,  $\tilde{K} \approx 0.1$ , and  $\tilde{g}_0 \approx 0.05\sqrt{C}$ . The slopes  $db(t)/dt|_{t=0}$  of four samples: 30 nm, 50 nm, and two 60 nm thick films (samples BS002, BS005, J033 and J038 respectively) are shown in the inset of Figure 4. We clearly see that the slope of the linear- $T$  anomaly increases with sheet resistance as predicted by Eq. (14), demonstrating the consistency of our theoretical description. Furthermore, the linear dependence of  $db(t)/dt|_{t=0}$  on the sheet resistance does not extrapolate to zero in the bulk limit ( $d \rightarrow \infty$ ), confirming again our theoretical result Eq. (14). However, fitting the data to Eq. (14) gives  $-db/dt = 0.4R_{\square}/R_Q + 0.44$ , i.e.,  $\tilde{g}_0 \approx 0.45$  and  $\tilde{K} \approx 0.4$ . These values exceed the ones found via our simplified approximation by a factor of about 4-10. Obtaining the correct numerical coefficients presumably requires including corrections neglected above, which is beyond the scope of this work.

## Discussion

In conclusion, we have conducted a systematic study of the critical current near  $B_{c2}(T = 0)$  in disordered a:InO films. These films are prototypical representatives of a variety of superconducting film in which the critical field shows an anomalous linear upturn as  $T \rightarrow 0$ . We uncovered a power-law dependence of  $j_c$  on magnetic field and extract the corresponding critical exponent. This previously unknown scaling property elucidates the origin of the 'critical field anomaly'—the strong deviation of  $B_{c2}$  from the mean-field result at the lowest temperatures. We have showed theoretically that the behavior of *both*  $B_{c2}(T)$  and  $j_c(B)$  can be attributed to the specific properties of the vortex-glass, which is characteristic state of disordered films in the presence of magnetic field. In particular, the anomalous dependence of  $B_{c2}$  on  $T$  is induced by a soft overdamped (bosonic) fluctuation mode of the vortex-glass. Although this mechanism is quite generally applicable for any disordered superconductor, both 2D and 3D, the magnitude of the effect is appreciable for superconductors with low superfluid density,  $\rho_s \xi_0 \leq T_{c0}$ , where phase fluctuations are strong [35].

Our analysis provides sharp predictions for  $B_{c2}(T)$  and  $j_c(B)$  which allows a clear distinction between the physical mechanisms in play. It would be very interesting to look for similar scaling in other superconducting films (in particular amorphous/non-amorphous) where a similar  $B_{c2}$  anomaly has been observed [3-8, 10-12]. A detailed measurement of the thickness and field dependence of the critical current could shed light on difference and similarities of the vortex-glass phases in conventional and also unconventional superconductors.

## Methods

**Derivation of the normalized slope  $db(t)/dt|_{t \rightarrow 0}$ .** Here we present the transformation between Eq. (13) and Eq. (14). Inserting Eq. (13) into  $b(t) = B_{c2}(T)/(-T_c dB_{c2}/dT|_{T=T_c})$  yields

$$\frac{b(0) - b(t)}{t} = \left[ 1 + \sqrt{1 + \frac{C_1^2 d^2}{a_0^2}} \right] \frac{\pi\chi}{24\rho_{s0}d} \frac{B_{c2}(0)}{|dB_{c2}/dT|_{T=T_c}}. \quad (15)$$

It remains only to determine  $B_{c2}$  in two limits,  $T \rightarrow 0$  and  $T \rightarrow T_c$ , starting with the latter. As discussed in the main text, the transition in the films is of the BKT type with the condition  $\rho_s(T, B_c) = \chi T/d$ . Near  $T_c$  the superfluid stiffness of a disordered superconductor is given by [36]

$$\rho_s(T, B) = \frac{\pi\sigma_n \hbar}{8Te^2} |\Delta(T, B)|^2. \quad (16)$$

The gap  $\Delta(T, B)$  near  $T_c$  can be found by minimizing the free energy in Eq. (2) without the gradient term,

$|\Delta|^2 = \alpha/2\beta$ . Here  $\alpha$  is giving by Eq. (3) which we expand to first order in  $B$ , and  $\beta = \nu\psi^{(2)}(1/2)/32\pi^2T^2$  [ $\psi^{(2)}(x) = d^2\psi(x)/dx^2$  is the second derivative of the digamma function]. Thus, in this limit the superfluid stiffness as a function of temperature and magnetic field is

$$\rho_s(T, B) = \frac{2\pi^2T\sigma_n h}{e^2\psi^{(2)}(1/2)} \left[ \ln \frac{T}{T_{c0}} + \psi' \left( \frac{1}{2} \right) \frac{eBD}{2\pi\hbar cT} \right]. \quad (17)$$

Inserting this expression into the BKT condition and taking a derivative with respect to the temperature yields

$$\left| \frac{dB_{c2}(T)}{dT} \right|_{T=T_c} = \frac{2\pi\hbar c}{eD\psi'(1/2)}. \quad (18)$$

The critical magnetic field at zero temperature, in contrast, is determined by the mean field condition  $\alpha = 0$

$$B_{c2}(T=0) = \frac{2\pi\hbar c}{eD} T_{c0} e^{\psi(1/2)}. \quad (19)$$

Using the expressions in Eqs. (18) and (19), we can write Eq (15) as

$$\frac{b(0) - b(t)}{t} = \left[ 1 + \sqrt{1 + \frac{C_1^2 d^2}{a_0^2}} \right] \frac{\pi\chi T_{c0}}{24\rho_{s0}d} \psi' \left( \frac{1}{2} \right) e^{\psi(1/2)}. \quad (20)$$

The final step in estimating  $b(t)$  is to find the ratio of  $\rho_{s0}$  to the mean-field transition temperature  $T_{c0}$ . For moderately disordered superconductors, in the absence of any pair-breaking mechanism, semiclassical theory yields [1, 36]

$$\rho_{s0} = \pi\Delta\hbar\sigma_n/4e^2 = 1.76\pi\hbar\sigma_n T_{c0}/4e^2. \quad (21)$$

We emphasize that the ratio  $\Delta/T_{c0}$  is expected to be reduced for strongly disordered superconductors [37–39], and as a consequence also  $\rho_{s0}/T_{c0}$  [34, 40, 41].

For ultra-thin films with  $d \ll a_0$  we find, using Eqs. (20) and (21),

$$\frac{b(0) - b(t)}{t} = 0.8 \frac{e^2}{\hbar\sigma_n d} = 0.4\pi \frac{R_{\square}}{R_Q} \equiv K \frac{R_{\square}}{R_Q}. \quad (22)$$

Here  $R_Q = h/4e^2$  is the quantum of resistance for electron pairs and we used  $\chi = 2/\pi$ , as appropriate for the two-dimensional limit. Since this result relies on Eq. 21 that overestimates the ratio  $\rho_{s0}/T_{c0}$ , we expect to experimentally observe larger values for  $K$ . For thick films with  $d \gg a_0$ , Eqs. (20) and (21) imply that  $|db/dt|$  grows linearly with  $R_{\square}/R_Q$ , i.e.,

$$\frac{b(0) - b(t)}{t} = \tilde{g}_0 \sqrt{\frac{e^2}{\hbar\sigma_n a_0}} + \tilde{K} \frac{R_{\square}}{R_Q}, \quad (23)$$

where  $\tilde{g}_0 \approx 0.05\sqrt{C}$ , and  $\tilde{K} \approx 0.1$ . Note that  $|db/dt|$  does not extrapolate to zero as  $R_{\square} = 1/\sigma_n d \rightarrow 0$ . Similar to

the result in the thin-film limit, the true numerical values of both  $\tilde{g}_0$  and  $\tilde{K}$  are expected to be larger due to the lower value of  $\rho_{s0}/T_{c0}$ . Moreover, as explained in the main text, the coefficients  $\tilde{g}_0$  and  $\tilde{K}$  can deviate from the values given by straightforward expansion of Eq. (20) for large  $d/a_0$ . Such a deviation would reflect higher-order corrections to  $\rho_s(T, B)$ , which may become important in thick films.

**Acknowledgments** We are grateful to Vadim Geshkenbein, Lev Ioffe, Thierry Klein and Mikhail Skvortsov for useful discussions. This work was supported by the Lab Alliance for Nanosciences and Energies for the Future (Lanef) and the H2020 ERC grant *QUEST* No. 637815. Research of M.V.F. was partially supported by the Russian Science Foundation grant # 14-42-00044 and Basic research program of the HSE.

\* Electronic address: benjamin.sacepe@neel.cnrs.fr

- [1] Abrikosov, A. A. and Gor'kov, L. P. Contribution to the theory of superconducting alloys with paramagnetic impurities. *Zh. Eksp. Teor. Fiz.* **39**, 1781 (1960) [*Sov. Phys. JETP* **12**, 1243 (1961)].
- [2] Maki, K. Critical Fluctuation of the Order Parameter in a Superconductor. I. *Prog. Theor. Phys.* **40**, 193–200 (1968).
- [3] Tenhover, M. and Johnson and W. L. and Tsuei, C. C. Upper critical fields of amorphous transition metal based alloys. *Solid State Commun.* **38**, 53–57 (1981).
- [4] Okuma, S. and Komori, F. and Ootuka, Y. and Kobayashi, S.-I. Superconducting properties of disordered films of Zn. *J. Phys. Soc. Jpn.* **52**, 2639–2641 (1983).
- [5] Hebard, A. F. and Paalanen, M. A. Pair-breaking model for disorder in two-dimensional superconductors. *Phys. Rev. B* **30**, 4063–4066 (1984).
- [6] Graybeal, J. M. and Beasley, M. R. Localization and interaction effects in ultrathin amorphous superconducting films. *Phys. Rev. B* **29**, 4167–4169 (1984).
- [7] Furubayashi, T. and Nishida, N. and Yamaguchi, M. and Morigaki, K. and Ishimoto, H. Superconducting properties of amorphous SiAu near metal-insulator transition. *Solid State Commun.* **55**, 513–516 (1985).
- [8] Nordström, A. and Dahlborg, U. and Rapp, Ö. Variation of disorder in superconducting glassy metals. *Phys. Rev. B* **48**, 12866–12873 (1993).
- [9] Sacépé, B. and Seidemann, J. and Ovadia, M. and Tamir, I. and Shahar, D. and Chapelier, C. and Strunk, C. and Piot, B. A. High-field termination of a Cooper-pair insulator. *Phys. Rev. B* **91**, 220508(R) (2015).
- [10] Ren, Z. and Kriener, M. and Taskin, A. A. and Sasaki, S. and Segawa, K. and Ando, Y. Anomalous metallic state above the upper critical field of the conventional three-dimensional superconductor *AgSnSe<sub>2</sub>* with strong intrinsic disorder. *Phys. Rev. B* **87**, 064512 (2013).
- [11] Bustarret, E. and Kačmarčík, J. and Marcenat, C. and Gheeraert, E. and Cytermann, C. and Marcus, J. and Klein, T. Dependence of the Superconducting Transition Temperature on the Doping Level in Single-Crystalline

- Diamond Films. *Phys. Rev. Lett.* **93**, 237005 (2004).
- [12] Xing, Y. and Zhang, H.-M. and Fu, H.-L. and Liu, H. and Sun, Y. and Peng, J.-P. and Wang, F. Lin, X. and Ma, X.-C. and Xue, Q.-K. and Wang, J. and Xie, X. C. Quantum Griffiths singularity of superconductor-metal transition in Ga thin films. *Science*, **350**, 542 (2015).
- [13] Spivak, B. and Zhou, F. Mesoscopic Effects in Disordered Superconductors near  $H_{c2}$ . *Phys. Rev. Lett.* **74**, 2800–2803 (1995).
- [14] Galitski, V. M. and Larkin, A. I. Disorder and Quantum Fluctuations in Superconducting Films in Strong Magnetic Fields. *Phys. Rev. Lett.* **87**, 087001 (2001).
- [15] Coffey, L. and Levin, K. and Muttalib, K. A. Upper critical field of strongly disordered three-dimensional superconductors: Localization effects. *Phys. Rev. B* **32**, 4382–4391 (1985).
- [16] Sadovskii, M. V. Superconductivity and localization. *Phys. Rep.* **282**, 225–348 (1997).
- [17] Smith, R. A. and Handy B. S. and Ambegaokar, V. Upper critical field in disordered two-dimensional superconductors. *Phys. Rev. B* **61**, 6352–6359 (2000).
- [18] Galitski, V. M. and Larkin, A. I. Superconducting fluctuations at low temperature. *Phys. Rev. B* **63**, 174506 (2001).
- [19] Galitski, V. Nonperturbative Microscopic Theory of Superconducting Fluctuations near a Quantum Critical Point. *Phys. Rev. Lett.* **100**, 127001 (2008).
- [20] Berezinskii, V. L. Destruction of long-range order in one-dimensional and two-dimensional systems having a continuous symmetry group I. Classical systems. *Zh. Eksp. Teor. Fiz.* **59**, 907–920 (1970) [*Sov. Phys. JETP* **32**, 493–500 (1971)].
- [21] Kosterlitz, J. M. and Thouless, D. J. Long range order and metastability in two dimensional solids and superfluids. (Application of dislocation theory). *J.Phys. C: Solid State Phys.* **5**, L124 (1972).
- [22] Larkin, A. I. and Ovchinnikov, Yu. N. Collective Pinning. *Physica B+C* **126**, 187–192 (1984).
- [23] Blatter, G. and Feigel'man, M. V. and Geshkenbein, V. B. and Larkin, A. I. and Vinokur, V. M. Vortices in high-temperature superconductors. *Rev. Mod. Phys.* **66**, 1125–1388 (1994).
- [24] Fisher, D. S. Flux-lattice melting in thin-film superconductors. *Phys. Rev. B* **22**, 1190–1199 (1980).
- [25] Fisher, D. S. and Fisher, M. P. A. and Huse, D. A. Thermal fluctuations, quenched disorder, phase transitions, and transport in type-II superconductors. *Phys. Rev. B* **43**, 130–159 (1991).
- [26] Campbell, A. M. The response of pinned flux vortices to low-frequency fields. *J.Phys. C: Solid State Phys.* **2**, 1492 (1969).
- [27] Campbell, A. M. The interaction distance between flux lines and pinning centres. *J.Phys. C: Solid State Phys.* **4**, 3186 (1971).
- [28] Coffey, M. W. and Clem, J. R. Unified theory of effects of vortex pinning and flux creep upon the rf surface impedance of type-II superconductors. *Phys. Rev. Lett.* **67**, 386 (1991).
- [29] Willa, R. and Geshkenbein, V. B. and Blatter, G. Probing the pinning landscape in type-II superconductors via Campbell penetration depth. *Phys. Rev. B* **93**, 064515 (2016).
- [30] Schneider, T. and Schmidt, A. Dimensional Crossover Scaling in the Layered xy-Model and  $^4\text{He}$  Films. *J. Phys. Soc. Jpn.* **61**, 2169–2172 (1992).
- [31] Ambegaokar, V. and Halperin, B. I. and Nelson, D. R. and Siggia, E. D. Dynamics of superfluid films. *Phys. Rev. B* **21**, 1806–1826 (1980).
- [32] Williams, G. A. Dimensionality crossover of the  $^4\text{He}$  superfluid transition in a slab geometry. *J. Low. Temp. Phys.* **101**, 415–420 (1995).
- [33] Schultka, N. and Manousakis, E. Crossover from two- to three-dimensional behavior in superfluids. *Phys. Rev. B* **51**, 11712–11720 (1995).
- [34] Misra, S. and Urban, L. and Kim, M. and Sambandamurthy, G. and Yazdani, A. Measurements of the Magnetic-Field-Tuned Conductivity of Disordered Two-Dimensional  $\text{Mo}_{43}\text{Ge}_{57}$  and  $\text{InO}_x$  Superconducting Films: Evidence for a Universal Minimum Superfluid Response *Phys. Rev. Lett.* **110**, 037002 (2013).
- [35] Emery, V. J. and Kivelson, S. A. Importance of phase fluctuations in superconductors with small superfluid density. *Nature*, **374**, 6521 (1995).
- [36] M. Tinkham, *Introduction to Superconductivity*, Dover, 1996.
- [37] Dynes, R. C. and White, A. E. and Graybeal, J. M. and Garno, J. P. Breakdown of Eliashberg Theory for Two-Dimensional Superconductivity in the Presence of Disorder. *Phys. Rev. Lett.* **57** 2195 (1986).
- [38] Valles, J. M. and Dynes, R. C. and Garno, J. P. Superconductivity and the electronic density of states in disordered two-dimensional metals. *Phys. Rev. B* **40** 6680–6683 (1989).
- [39] Finkel'stein, A. M. Suppression of superconductivity in homogeneously disordered systems. *Physica B* **197**, 636–648 (1994).
- [40] Feigel'man, M. V. and Ioffe, L. B. and Kravtsov V. E. and Cuevas, E. Fractal superconductivity near localization threshold. *Ann. Phys.* **325**, 1390–1478 (2010).
- [41] Feigel'man, M. V. and Ioffe, L. B. Superfluid density of a pseudogapped superconductor near the superconductor-insulator transition. *Phys. Rev. B* **92**, 100509 (2015).